

Purchase  
Information

Information  
pour  
acheter

Titles  
Titres

←  
Article

→  
Article



**Geological Survey  
of Canada**

**CURRENT RESEARCH  
2001-A12**

***Ground-magnetic investigations of Cenozoic  
structures in the northern Cascadia forearc,  
British Columbia***

***C. Lowe, J. Baker, and J.M. Journeay***



Natural Resources  
Canada

Ressources naturelles  
Canada

Canada

# CURRENT RESEARCH RECHERCHES EN COURS 2001

Purchase  
Information

Information  
pour  
acheter

Titles  
Titres

←  
Article

→  
Article



©Her Majesty the Queen in Right of Canada, 2001  
Catalogue No. M44-2001/A12E-IN  
ISBN 0-662-29792-X

Available in Canada from the  
Geological Survey of Canada Bookstore website at:  
<http://www.nrcan.gc.ca/gsc/bookstore> (Toll-free: 1-888-252-4301)

A copy of this publication is also available for reference by depository  
libraries across Canada through access to the Depository Services Program's  
website at <http://dsp-psd.pwgsc.gc.ca>

Price subject to change without notice

**All requests for permission to reproduce this work, in whole or in part, for purposes of commercial use, resale, or redistribution shall be addressed to: Earth Sciences Sector Information Division, Room 200, 601 Booth Street, Ottawa, Ontario K1A 0E8.**



## Ground-magnetic investigations of Cenozoic structures in the northern Cascadia forearc, British Columbia

**C. Lowe, J. Baker, and J.M. Journeay<sup>1</sup>**  
*GSC Pacific, Sidney*

*Lowe, C., Baker, J., and Journeay, J.M., 2001: Ground-magnetic investigations of Cenozoic structures in the northern Cascadia forearc, British Columbia; Geological Survey of Canada, Current Research 2001-A12, 16 p.*

<sup>1</sup> GSC Pacific, Vancouver  
101-605 Robson Street  
Vancouver, B.C. V6B 5J3

### **Abstract**

*Accurate delineation of active structures is a critical component in improved seismic hazard models of the northern Cascadia forearc. To date, young faults in this region have been mapped directly through geological methods and indirectly through expensive seismic methods. We report findings of pilot ground magnetic surveys conducted across five Cenozoic structures in the forearc. The survey objective was to determine if high-resolution aeromagnetics could provide a faster and less expensive method of delineating the structures than currently exists.*

*Results show recent deformation resulted in depletion of magnetic minerals from most fault zones. However, as the undeformed sedimentary rocks surveyed are only weakly magnetic, the magnetization contrast created by this loss was, in most cases, insufficient to generate a clear magnetic anomaly. However, moderately to highly magnetic crystalline rocks underlie much of the frontal arc and western forearc. If similarly deformed, structures cutting these rocks have the potential to generate large magnetic anomalies.*



## Résumé

*La délimitation exacte des structures actives est un élément essentiel pour améliorer les modèles de risques sismiques dans l'avant-arc septentrional de Cascadia. Jusqu'à ce jour, les jeunes failles présentes dans cette région ont été cartographiées directement à l'aide de méthodes géologiques et indirectement en appliquant des méthodes sismiques coûteuses. Nous présentons les résultats de levés magnétiques terrestres pilotes effectués dans cinq structures du Cénozoïque dans l'avant-arc. L'objectif était de déterminer si les levés aéromagnétiques haute résolution constituaient une méthode plus rapide et économique que celles appliquées actuellement pour délimiter les structures.*

*Les résultats ont révélé que la déformation récente a entraîné un appauvrissement en minéraux magnétiques dans la plupart des zones de failles. Toutefois, comme les roches sédimentaires non déformées examinées ne sont que faiblement magnétiques, le contraste de la magnétisation créé par cet appauvrissement a été insuffisant, dans la plupart des cas, pour générer une anomalie magnétique nette. Cependant, des roches cristallines modérément à très magnétiques sont présentes dans une grande partie de l'avant-arc septentrional et de l'avant-arc occidental. Dans l'éventualité où elles ont été l'objet d'une déformation similaire, les structures qui traversent les roches cristallines seraient susceptibles de produire de grandes anomalies magnétiques.*

## INTRODUCTION

Much of the densely populated area of southwestern British Columbia and the Pacific Northwest lies within the Cascadia forearc. This forearc, which extends from the Juan de Fuca trench to the Neogene volcanic front, is subject to a variety of geological hazards, including earthquakes (**Fig. 1**). Two recent, widely felt, shallow earthquakes located within the forearc (M=4.6 in 1997 near Vancouver and M=5.0 in 1995 near Seattle) are reminders of the seismic potential of this region. However, models that accurately explain observed variations in the spatial and temporal distribution of stress within the



forearc are lacking, and consequently our capacity for predicting seismic hazard remains limited. Geodetic observations of contemporary surface deformation (Dragert et al., 1994; Dragert and Hyndman, 1995; Henton et al., 1998) indicate that maximum crustal shortening is margin-normal. Focal-mechanism solutions of recent earthquakes in southwestern British Columbia (Wang et al., 1995; Cassidy et al., in press) and Puget Sound (Ma et al., 1991), shear-wave anisotropy investigations in southwestern British Columbia (Cassidy and Bostock, 1996), as well as borehole breakout data from wells in western Oregon and Washington (Werner et al., 1991; Magee and Zoback, 1992) indicate that the direction of maximum crustal stress is horizontal and margin-parallel.

Geological evidence of Neogene deformation provides important information on the regional stress regime at longer time scales than the geophysical measurements and studies just described. In the southern Cascadia forearc of Washington and Oregon, Johnson et al. (1994), Snavely and Wells (1996), and McCrory (1996) document geological evidence of active east-trending uplifts and associated thrust or reverse faults consistent with north-south shortening. Although published reports of young geological deformation in the northern Cascadia forearc are few, Journeay and Morrison (1999) document a Late Oligocene–Early Miocene transition from margin-normal shortening to dextral strike-slip faulting and associated margin-parallel extension, but as yet, there is no evidence of recent margin-parallel shortening in this region.

In addition, the relationship between the location of earthquakes and mapped Neogene structures remains poorly constrained in the northern Cascadia forearc. Here, most of the mapped Cenozoic faults are exposed along the shorelines of Vancouver Island, the Gulf Islands, and the lower mainland (Journeay and Morrison, 1999), but the presence of sedimentary and glacial deposits, water, vegetation, and urban development has prohibited extending many of these structures inland. Also, two thirds of the mapped structures lack sense-of-motion indicators. Indirectly, neotectonic structures in this region have been delineated using the following geophysical methods: the interpretation of offshore seismic profile



data (Mosher et al., 1997; Mosher et al., 2000), and accurate location and focal mechanism studies of earthquakes (Cassidy et al., in press). Geological mapping is a slow process and seismic methods are expensive.

Here we report the Phase I findings of ground magnetic surveys conducted across five Cenozoic, high-angle, brittle structures in the Gulf Islands region of the forearc. The majority of the faults surveyed juxtapose sedimentary rocks against sedimentary rocks and the objective of the surveys was to determine if the structures have an associated magnetic signature. If a well defined magnetic signature could be established, then low-level high-resolution aeromagnetic surveying could be used to provide a rapid and inexpensive method of mapping these features.

A lateral contrast in magnetic susceptibility is a prerequisite for the generation of any magnetic anomaly. Thus a fault that juxtaposes units with contrasting magnetic susceptibilities will have an associated magnetic signature, typically a steep gradient. In the southern Cascadia forearc, young faults that juxtapose high-susceptibility volcanic rocks with low-susceptibility sedimentary units are readily imaged in aeromagnetic data as linear zones of steep magnetic gradient (Blakely et al., 1995). Where a fault cuts a single rock unit, a magnetic anomaly is not normally observed unless deformation, metamorphism, and/or the migration of fluids in the fault zone lead to the development or removal of magnetic minerals.

The majority of mapped Cenozoic structures in the northern Cascadia forearc cut imbricated Late Cretaceous–Early Tertiary clastic successions in the Strait of Georgia and adjacent coastal regions. Consequently, our Phase I pilot ground magnetic surveys were conducted over structures cutting these clastic units. Although most sedimentary rocks are weakly magnetic, recent advances in acquisition technologies (including increased instrument sensitivities and real-time differential GPS positioning) coupled with improvements in airborne-survey design and data processing now permit very subtle contrasts in magnetic susceptibility to be imaged aeromagnetically. For example, Grauch and Millegan (1998)



successfully used high-resolution aeromagnetics to locate intrabasinal faults in the Albuquerque Basin, New Mexico. There, brecciation and chemical changes along active fault zones led to a loss of magnetization and the faults were clearly imaged in aeromagnetic maps as lows with flanking highs. However, the amplitudes of the fault-associated anomalies ranged from just 2nT to 10 nT at 100 m altitude, implying that depletions in magnetic minerals within the fault zones were small. Similarly, if the susceptibility differences between clastic units in our study area proved negligible, then stabilization of secondary magnetic minerals or alternatively depletion of primary magnetic minerals from the fault regions would be a necessary prerequisite for the faults to have an associated magnetic signature.

## GEOLOGY OF THE STUDY AREA

The northern Cascadia forearc (**Fig. 1**) includes imbricated continental-margin sequences in the forearc accretionary complex, as well as exhumed preTertiary crystalline rocks on Vancouver Island and the southwestern Coast Mountains. Overlying the crystalline rocks in the Strait of Georgia and adjacent coastal areas are imbricated Late Cretaceous–Early Tertiary clastic successions of the Nanaimo Group and Huntington (Canada)/Chuckanut (United States) Formation. The Nanaimo Group, which in places is more than 4 km thick, has been subdivided into eleven formations, five of which (Haslam, Extension, Pender, Protection, and DeCourcy) were traversed in the surveys described herein. These five formations include massive and bedded sandstone, marine mudstone, boulder conglomerate, and turbidite, in large part derived from the erosion of intermediate and mafic crystalline rocks in the Coast Plutonic Complex to the east (Mustard, 1994). The Fulford fault zone juxtaposes these clastic rocks with polydeformed meta-andesite and dacite of the Carboniferous Sicker Group.



The main structural control on the sub-Nanaimo Group rocks, and to some extent on the Nanaimo Group itself, is southwest- to west-vergent thrusting that took place from Late Jurassic to Holocene time in response to underthrusting of the Farrallon–Kula (now Juan de Fuca) oceanic plates beneath the North American Plate. The Cenozoic faults surveyed in this study occur in widely distributed networks of north-west-, north- and northeast-trending, high-angle, brittle faults, the majority of which record evidence of either strike-slip or normal dip-slip displacement (Journeay and Morrison, 1999). Within any network, the majority of structures are marked by 1 to 5 m wide zones of fracturing, brecciation, localized fault gouge development, and associated hydrothermal alteration. Where measurable, displacements are typically small, on the order of 10 m or less, and appear to be partitioned along either northwest-trending, dextral strike-slip or north- and northeast-trending, dip-slip normal faults. The larger faults record offsets of 500 m or more, and can be traced along strike for several kilometres. In a number of cases, such as the Fulford and Pender Island fault zones investigated in this study, anastomosing networks of brittle structures, occurring in zones up to 1 km wide, have been mapped. In these cases, individual structures within the network have characteristics and scales comparable to those described above. Motion is commonly transferred from one fault string to another in the network such that, at any location along the fault zone, only one string is active. Although the precise timing of motion on these Cenozoic faults is uncertain, they cut folds and thrusts of the Gulf Island thrust system that deform Paleogene rocks, and as such they must be Paleogene or younger.

## EXISTING MAGNETIC DATA

Prior to the surveys described herein, regional aeromagnetic data were available for the study area. These regional data were acquired on north-south flight lines that were spaced 1200 m apart and flown at a barometric altitude of 762 m. Consequently, most small-scale structures described above





are not resolved by the data. However, the data do provide good resolution of the regional geology. In particular, they show that the Nanaimo and Sicker groups cannot be distinguished magnetically as they have comparable magnetic anomaly amplitudes and gradients.

Paleomagnetic investigations of the Nanaimo Group indicate that magnetite is the dominant magnetic mineral in all formations (Enkin et al., in press). The magnetite typically consists of large multidomain grains with very low magnetic stability, that is, it is readily remagnetized. Their analysis also shows that, for all formations, the Koenigsberger ratios (i.e. the ratio of remanent to induced magnetizations) are very low.

## SURVEY METHODOLOGY

Ground magnetic and in situ magnetic susceptibility measurements were conducted across five Cenozoic structures on Saltspring and Pender islands (**Fig. 1**). In the case of three of the structures (1, 2, 3, Fig. 1), the objective was to determine if individual fault strands had an associated magnetic signature. In the other two cases (4, 5, Fig. 1), the objective was to determine if the zone encompassing a network of fault strands had an associated magnetic signal. Magnetic measurements were conducted using a Geonics GEM Systems proton precession magnetometer with an accuracy of 1 nT. In all cases, the magnetic sensor was located 2 m above ground level. The surveys were conducted between 25 August and 11 September 1999, during periods of low magnetic disturbance. The small diurnal contribution to measured values was subsequently removed using data from the Victoria international magnetic observatory. An average of 10 in situ magnetic susceptibility measurements was measured at selected outcrop localities along each traverse using an Exploranium KT-9 Kappameter.



## *Northwest-trending dip-slip fault, Welbury Bay, Saltspring Island*

This northwest-trending dip-slip structure cuts homogeneous, coarse-grained sandstone of the De Courcy Formation. It is exposed at the head of Welbury Bay and on the south and north shores of Long Harbour (1, **Fig. 1**). The fault zone, which is just less than 1 m wide, is characterized by intense fracturing, brecciation, and associated hydrothermal alteration.

A 23 m magnetic traverse at a station spacing of 33 cm was conducted across the fault at Welbury Bay (**Fig. 2a**). Measured magnetic values varied from a minimum of 55 630 nT at the centre of the fault zone to a maximum of 55 696 nT approximately 6 m to the east. Values were relatively low in an 8 m zone around the fault and higher and more varied farther east and west. Magnetic susceptibility values along this traverse were also a minimum ( $0.1 \times 10^{-3}$  SI) at the fault zone and increased to the east (Fig. 2a). The maximum measured magnetic susceptibility was  $1.93 \times 10^{-3}$  SI at 9.3 m from the fault. Although susceptibility values also increased to the west, they did not do so systematically, and measured values near the western end of the transect were only slightly higher ( $0.22 \times 10^{-3}$  SI) than those observed in the fault zone.

Magnetic susceptibility was also measured across this structure at the Long Harbour outcrop locality where the fault cuts a coarse-grained sandstone unit. Here, measured values were consistently negative within and to the east of the fault zone and consistently positive to the west of the fault zone (**Fig. 2b**). In general, negative susceptibility values indicate an absence of iron oxides and the predominance of diamagnetic minerals such as quartz, apatite, orthoclase, and zircon.



## *Northeast-trending dip-slip structures on Athol Peninsula, Saltspring Island*

Journeay and Morrison (1999) mapped two northeast-trending dip-slip structures on the shorelines of the Athol and Nose Point peninsulas, Saltspring Island (2, 3, **Fig. 1**). The westernmost of the two structures (2, **Fig. 1**) is composite and composed of (at least) two distinct fault strands; a discrete, 30 to 40 cm wide zone of brecciation, and a significantly wider (10–20 m) zone of fracturing. Susceptibility measurements conducted across both strands (**Fig. 3a, b**) are comparable, ranging from  $0.6 \times 10^{-3}$  SI to  $3.3 \times 10^{-3}$  SI, with the minimum in each case occurring at the fault zone.

The easternmost of the two structures (3, **Fig. 1**) outcrops approximately 500 m to the southeast on the southern shore of Athol Peninsula, as well as on the southern shore of Long Harbour. It is characterized by a 1.5 m wide zone of intense fracturing and hydrothermal alteration. Magnetic susceptibility measurements across the fault strand at the former locality (**Fig. 3c**) have a very small range ( $0.42 \times 10^{-3}$  to  $1.51 \times 10^{-3}$  SI); nonetheless the measured minimum value is found at the fault.

Extremely limited access prohibited detailed shoreline magnetic traverses of these structures. However, a 1.2 km magnetic traverse, at a station interval of 3 m, was conducted across both structures on the Athol Peninsula road leading to Scott Point (**Fig. 4**). Magnetic values ranged from a minimum of 55 447 nT near the northwestern end of this traverse to a maximum of 55 865 nT near the southwestern end and, in general, are more varied toward the northern end of the traverse. Magnetic susceptibility measurements were also taken at outcrop localities along this traverse (**Fig. 4**). Values range from a minimum of  $1.87 \times 10^{-3}$  SI to a maximum of  $5.83 \times 10^{-3}$  SI, with generally higher values over the northern half of the profile. The inferred locations of the two northeast-trending fault structures along this traverse are also shown in **Figure 4**.



### *Northeast-trending brittle fault, Pender Island*

Two magnetic traverses were conducted across a northeast-trending brittle fault on North Pender Island. This fault is exposed on the shoreline just east of Boat Nook (4, **Fig. 1**) where it records a dip-slip sense of displacement. Inland, the fault is inferred from stratigraphic offsets of the Extension, Pender, and Protection formations.

Along both traverses, magnetic measurements were conducted at 5 m intervals in a zone approximately 1 km wide centred on the inferred fault location and at 10 m intervals outside this zone. Measured values are comparable along both traverses (**Fig. 5**). In general, values are more consistent over sandstone units exposed at the southeastern end of these transects compared with those observed over conglomerate units exposed farther to the northwest. The inferred location of the fault does not correspond with a distinct anomaly on either traverse. Magnetic susceptibilities were measured at 13 outcrop localities along the southern traverse (Fig. 5). In general, the range of individual values in sandstone units was very small ( $0-3 \times 10^{-3}$  SI), whereas individual values were significantly more varied in conglomerate units, with some clasts yielding negative values and others yielding values as large as  $19 \times 10^{-3}$  SI. Overall however, average values were slightly higher in sandstone units. The lowest measured average susceptibility value was found 0.95 km east of the inferred fault location. There was no outcrop at the inferred fault location on this traverse.

### *Fulford fault zone, Saltspring Island*

The Fulford fault zone is defined by a network, in places up to 1 km wide, of southwest-dipping, ductile and brittle shear zones with subhorizontal lineations, and asymmetric fault-zone fabrics that record an episodic history of oblique, top-to-the-northeast, dextral strike-slip displacement of some 6 km



(Journeay and Morrison, 1999). Magnetic measurements were taken on all accessible public roads and beaches that crossed this structure at a steep angle (5, **Fig. 1**). The Fulford Harbour transect was the longest and the Burgoyne Bay transect, the shortest (Fig. 1). In each case, the station spacing was 5 m in a 1 km zone about the centre of the inferred structure and 10 m outside this zone. All transects, reprojected onto a straight line, showed an increase in average magnetic anomaly values toward the north (**Fig. 6**). In the cases of the Jones–Fulford Ganges and Furness–Fulford Ganges transects, this change occurred very close to the inferred location of the centre of the structure, whereas along the other two transects the change occurred farther north (~500 m farther north on the Fulford Harbour transect, and ~200 m farther north on the Burgoyne Bay transect). The amplitude of the increase averaged 130 nT (Fig. 6). A similar northward increase in anomaly values is observed in the regional aeromagnetic data.

Measured susceptibilities in the Sicker Group were comparable to those reported above for the Nanaimo Group, i.e. approximately  $3 \times 10^{-3}$  SI in undeformed rocks and about  $1 \times 10^{-3}$  SI in deformed zones. A large outcrop of Saltspring Intrusions exposed at the north end of the Fulford Ganges transect had an average magnetic susceptibility of just  $0.33 \times 10^{-3}$  SI. As the exposed lithological units cannot account for the observed increase in anomaly values beneath the northern part of Saltspring Island, a buried magnetic body is inferred to exist in this region.

With the exception of the large outcrop of the Saltspring Intrusions at the north end of the Fulford–Ganges road, no magnetic susceptibility measurements were taken along the three westernmost transects crossing this structure because of the lack of available outcrop. Numerous susceptibility measurements were taken along the northern part of the Fulford Harbour transect; they ranged from a minimum of  $0.01 \times 10^{-3}$  SI close to the fault to a maximum of  $3.29 \times 10^{-3}$  SI approximately 0.8 km to the north.



## SUMMARY

Detailed magnetic susceptibility measurements and ground magnetic surveys were conducted across a number of individual fault strands and fault networks in the northern Cascadia forearc. The surveyed structures displace Late Cretaceous–Early Tertiary clastic rocks of the basal Nanaimo Group and polydeformed meta-igneous units of the Carboniferous Sicker Group. Results show that undeformed rocks in both groups are characterized by low average magnetic susceptibility values, typically  $<5 \times 10^{-3}$  SI. Along and adjacent to individual fault strands susceptibility values are usually lower still (i.e.  $<1 \times 10^{-3}$  SI). This suggests that deformation was accompanied by depletion of magnetic minerals, i.e. magnetite. However, excepting the northwest-trending structure exposed at Welbury Bay, Saltspring Island magnetic-field measurements across individual fault strands and across networks of faults show no clear associated reduction in intensity. This implies that the volume of magnetite removed from individual fault strands and from the zones encompassing fault networks is small, such that the resulting magnetization contrast is insufficient to generate a distinct magnetic anomaly.

Synthetic models show that a 10 m wide vertical fault zone (magnetic susceptibility of  $1 \times 10^{-3}$  SI) having a 2 km depth extent that cuts a homogeneous rock unit (magnetic susceptibility of  $4 \times 10^{-3}$  SI) generates a negative magnetic anomaly with a peak amplitude of just -30 nT. Such an anomaly is significantly smaller than the observed variation (typically on the order of 100–200 nT) in ground magnetic intensity across any of the rock units surveyed away from the deformed zones. Similarly, a 1 km wide zone of deformation of similar magnetic contrast would generate a peak anomaly of just -60 nT (**Fig. 7**), also insufficient to produce a recognizable anomaly. Consequently, we conclude that magnetic data cannot be used to reliably identify Cenozoic structures that cut and juxtapose these clastic and meta-igneous rock units.



To date, very few Cenozoic structures have been mapped in the older crystalline rocks exposed on Vancouver Island. However, Cenozoic faults which juxtapose low susceptibility (typically  $<5 \times 10^{-3}$  SI; Hunter et al., 1995) sediments of the Fraser Lowlands with higher susceptibility (typically  $>20 \times 10^{-3}$  SI; Coles and Currie, 1977) rocks of the Coast Plutonic complex have been mapped in the frontal arc east of the Georgia Basin (Fig. 1; Journeay and Morrison, 1999). Synthetic models show that the simple juxtaposition of rocks with these magnetic susceptibilities should generate magnetic anomalies in excess of 500 nT (Fig. 7). Such anomalies should be readily detected in ground and low-level airborne surveys. Similarly, significant depletion and/or complete removal of magnetite from fault zones cutting these crystalline units also has the potential to generate significant magnetic anomalies. Surveys of mapped structures in the frontal arc are planned to assess the application of magnetic methods to fault delineation there.

## ACKNOWLEDGMENTS

The critical reviews of Ralph Currie and Randy Enkin were very much appreciated. Richard Franklin assisted with drafting Figure 1.

## REFERENCES

**Blakely, R.J., Wells, R.R., Myelin, T.G., Main, I.W., and Beeston, M.H.**

1995: Tectonic setting of the Portland-Vancouver area, Oregon and Washington: constraints from low-altitude aeromagnetic data; Bulletin, Geological Society of America, v. 107, p. 1051–1062.

**Brandon, M.T., Cowan, D.S., and Vance, J.A.**

1988: The Late Cretaceous San Juan thrust system, San Juan Islands, Washington; Geological Society of America, Special Paper 221, 81 p.

**Cassidy, J.F. and Bostock, M.G.**

1996: Shear-wave splitting above the subducting Juan de Fuca plate; *Geophysical Research Letters*, v. 23, p. 941–944.

**Cassidy, J.F., Rogers, G.C. and Waldhauser, F.**

in press: Seismic evidence for active faulting beneath the Strait of Georgia; *Bulletin, Seismological Society of America*.

**Coles, R.L. and Currie, R.G.**

1977: Magnetic anomalies and rock magnetizations in the southern Coast Mountains, British Columbia: possible relation to subduction; *Canadian Journal of Earth Sciences*, v. 14, p. 1753–1770.

**Dragert H. and Hyndman R.D.**

1995: Continuous GPS monitoring of elastic strain in the northern Cascadia subduction zone; *Geophysical Research Letters*, v. 22, p. 755–758.

**Dragert, H., Hyndman, R.D., Rogers, G.C., and Wang, K.**

1994: Current deformation and the width of the seismogenic zone of northern Cascadia subduction thrust; *Journal of Geophysical Research*, v. 99, p. 653–668.

**England, T.D.J. and Calon, T.J.**

1991: The Cowichan fold and thrust system, Vancouver Island, southwestern British Columbia; *Geological Society of America Bulletin*, v. 103, p. 336–362.

**Enkin, R.J., Baker, J., and Mustard, P.S.**

in press: Paleomagnetism of the Lake Cretaceous Nanaimo Group, Insular and Coast Belt, Southern Canadian Cordillera, *Canadian Journal of Earth Sciences*.

**Grauch, V.J.S. and Millegan, P.S.**

1988: Mapping intrabasinal faults from high-resolution aeromagnetic data; *The Leading Edge*, p. 53–55.

**Henton, J., Dragert, H., Hyndman, R.D., and Wang, K.**

1998: Geodetic monitoring of crustal deformation on Vancouver Island; *EOS Transactions, American Geophysical Union*, v. 79, no. 45; Fall Meeting Supplement F192.

**Hunter, J.A., Burns, R.A., Good, R.L., Wang, Y., and Evans, M.E.**

1995: Borehole magnetic susceptibility measurements in unconsolidated overburden of the Fraser River delta, British Columbia; *in Current Research 1995-E*; Geological Survey of Canada, p. 77–82.





**Johnson, S.Y., Potter, C.J.M., and Armentrout, J.M.**

1994: Origin and evolution of the Seattle Fault and central Puget Sound, Washington — implications for earthquake hazards; *Bulletin, Geological Society of America*, v. 111, p. 1042–1053.

**Journey, J.M. and Morrison, J.**

1999: Field investigation of Cenozoic structures in the northern Cascadia forearc, southwestern British Columbia; *in* Current Research 1999-A; Geological Survey of Canada, p. 239–250.

**Journey, J.M., Sander, C., Van-Konijnenburg, J.H., and Jaasma, M.**

1992: Fault systems of the eastern Coast Belt, southwestern British Columbia; *in* Current Research, Part A; Geological Survey of Canada, Paper 92-1A, p. 225–236.

**Ma, L., Crossan, R., and Ludwin, R.**

1991: Focal mechanisms of western Washington earthquakes and their relationship to regional tectonic stress; United States Geological Survey, Open File 91-144-D, 28 p.

**Magee, M.E. and Zoback, M.L.**

1992: Wellbore breakout analysis for determining tectonic stress orientations in Washington State; United States Geological Survey Open File Report 92-715, 56 p.

**McCrory, P.A.**

1996: Tectonic model explaining divergent contraction directions along the Cascadia subduction margin, Washington; *Geology*, v. 24, p. 929–932.

**Mosher, D.C., Cassidy, J.F., Lowe, C., Mi, Y., Hyndman, R.D., and Rogers, G.C.**

2000: Neotectonics in the Strait of Georgia: first tentative correlation of seismicity with shallow geological structure in southwestern British Columbia; *in* Current Research 2000-A22, 9 p. (online; <http://www.nrcan.gc.ca/gsc/bookstore>).

**Mosher, D.C., Hewitt, A.T., and Hamiltom, T.G.**

1997: Neotectonic activity in the eastern Juan de Fuca Strait: quantitative seismic reflection mapping; *in* Program with Abstracts, American Geophysical Union Annual Meeting, 1997, San Francisco, California, T11B-12.

**Mulder, T.L.**

1995: Small earthquakes in southwestern British Columbia (1975–1991); M.Sc. Thesis, University of Victoria, Victoria, British Columbia.

**Mustard, P. S.**

1994: The Upper Cretaceous Nanaimo Group, Georgia Basin; *in* Geological Hazards of the Vancouver Region, Southwestern British Columbia, (ed.) J.W.H. Monger; Geological Survey of Canada, Bulletin 481, p. 27–96.

**Prieto, C.**

1997: Gravity/magnetic signatures of various geologic models — an exercise in pattern recognition, *in* Geologic Applications of Gravity and Magnetism, (ed.) R.I. Gibson and P.S. Milligan; SEG Geophysical Reference Series, no. 8, p. 20–27.

**Snavely, P.D., Jr. and Wells, R.R.**

1996: Cenozoic evolution of the continental margin of Oregon and Washington; *in* Assessing Earthquake Hazard and Reducing Risk in the Pacific Northwest, (ed.) A.M. Rogers, T.J. Walsh, W.J. Kockelman, and G.R. Priest; United States Geological Survey, Professional Paper 1560, p. 161–182.

**Wang, K., Mulder, T., Rogers, G.C., and Hyndman, R.D.**

1995: Case for very low coupling stress on the Cascadia subduction fault; *Journal of Geophysical Research*, v. 100, p. 907–918.

**Werner, K.S., Graven, E.P., Berkamn, T.A., and Parker, M.J.**

1991: Direction of maximum horizontal compression in western Oregon determined from borehole breakouts; *Tectonics*, v. 10, p. 948–958.

---

Geological Survey of Canada Project 910027-01

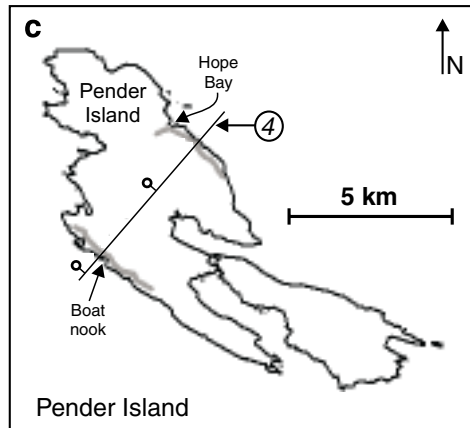
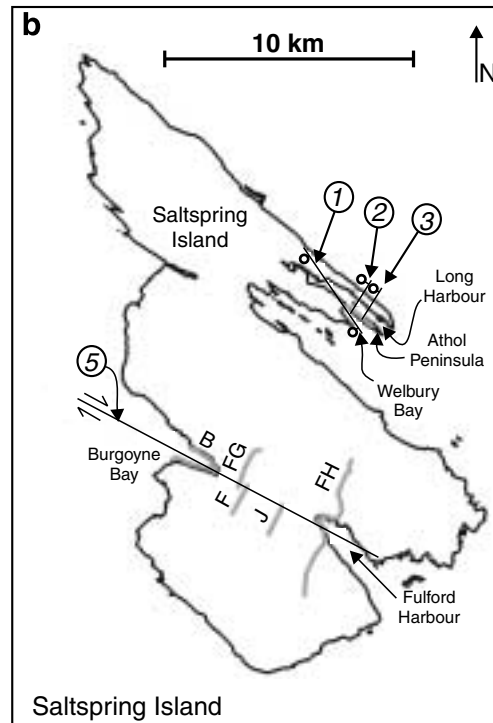
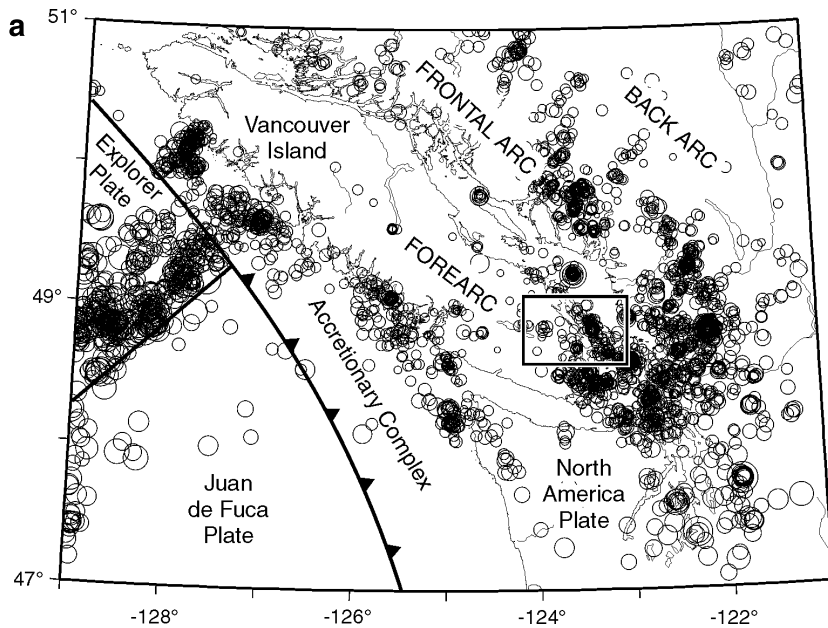


**Figure 1.** a) Tectonic setting of the study area within the northern Cascadia forearc. Circles show the locations of all earthquakes that occurred between 1975 and 1991 at depths <30 km (Mulder, 1995); circle size is proportional to earthquake magnitude (data incomplete in the United States); b) Saltspring Island; and c) Pender Island. In b) and c), the location and sense of motion of the five structures investigated are indicated with thin black lines and the locations of the magnetic surveys conducted across them, in thick grey lines. Abbreviations in b) are as follows: B, Burgoyne Bay; FG, Fulford Ganges; F, Furness; J, Jones; FH, Fulford Harbour.

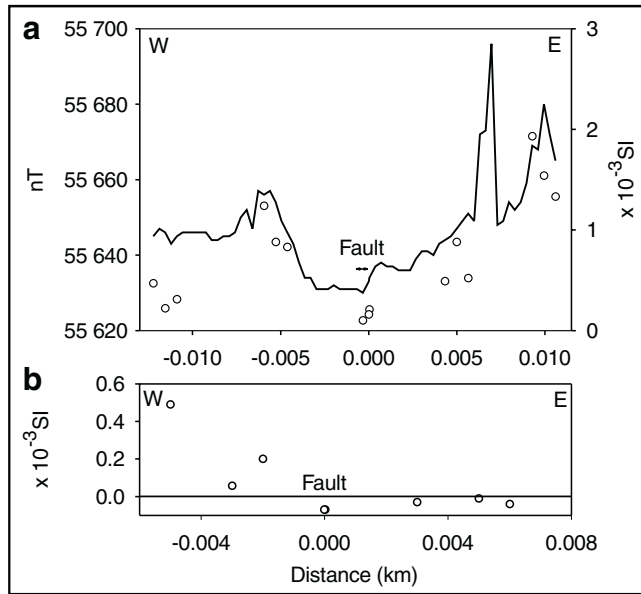


**Figure 2. a)** Magnetic traverse (solid line) across the northwest-trending dip-slip fault exposed at Welbury Bay, Saltspring Island (1, Fig. 1). Magnetic susceptibility values are plotted with open circles. **b)** Magnetic susceptibility measurements across the same structure where it is exposed on the north shore of Long Harbour.

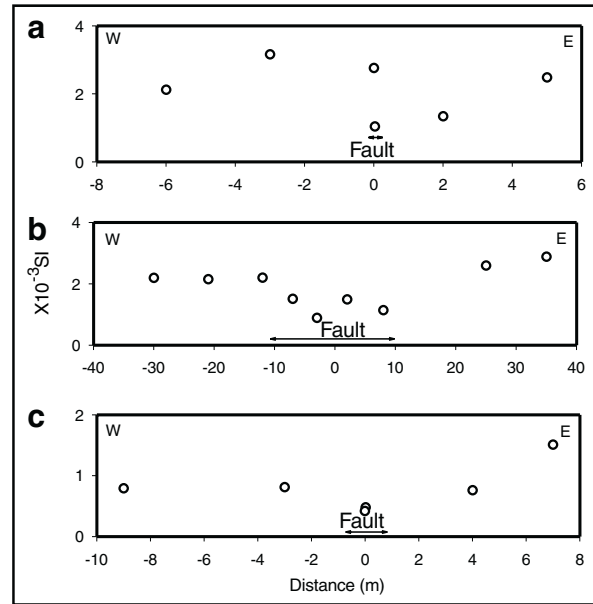


**Figure 3.** Averaged magnetic susceptibility values across two northeast-trending dip-slip structures on Saltspring Island. The westernmost of the two structures (2, Fig. 1) comprises at least two distinct strands, one of which is approximately 30 to 40 cm wide (a) and the other, 10 to 20 m wide (b). The eastern structure (3, Fig. 1) consists of a single fault strand approximately 0.5 m wide (c).

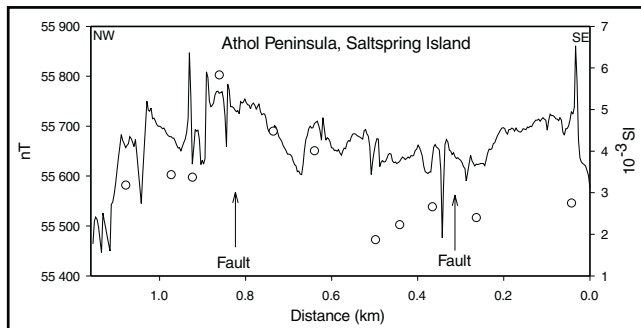


**Figure 4.** Magnetic measurements (solid line) conducted across two northeast-trending dip-slip structures on Athol Peninsula, Saltspring Island (2, 3, Fig. 1). Magnetic susceptibility values for outcrop localities along the traverse are plotted as open circles.

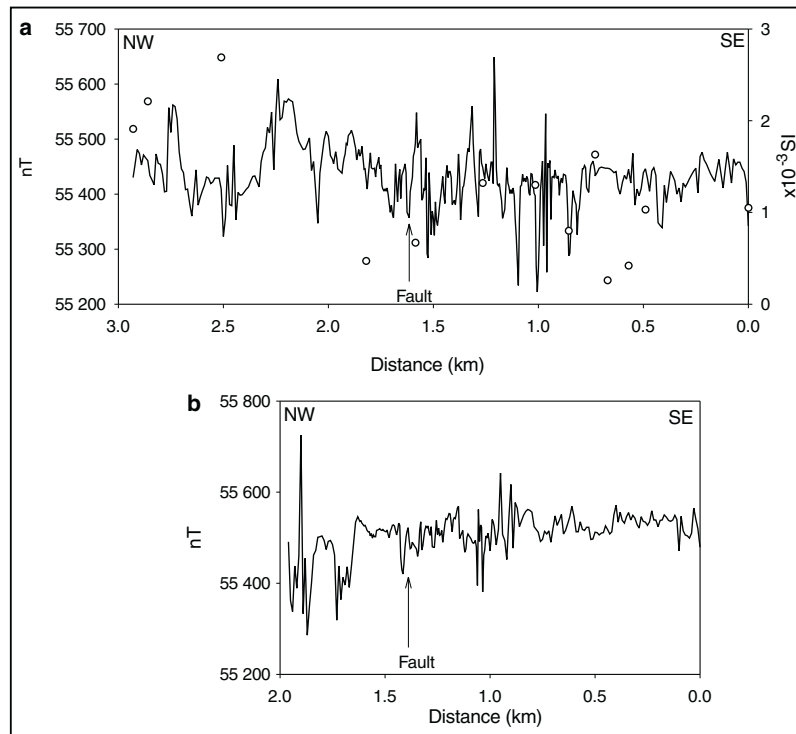


**Figure 5.** Magnetic measurements (solid lines) across a northeast-trending dip-slip structure on Pender Island (4, Fig. 1). **a)** Traverse near Boat Nook Bay; **b)** traverse near Hope Bay. The inferred location of the fault along each traverse is indicated. Magnetic susceptibility values are plotted as open circles.

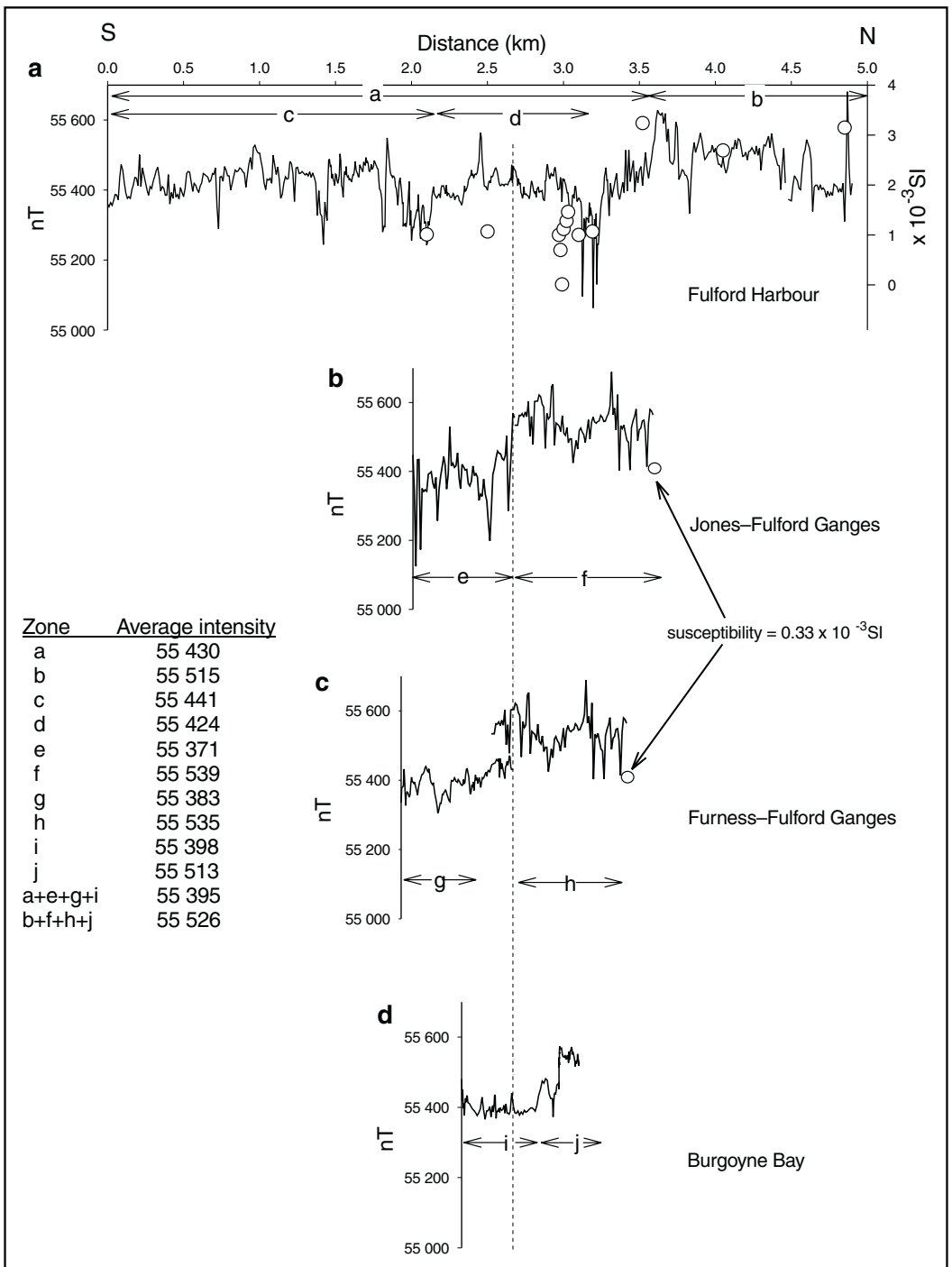


**Figure 6.** Magnetic measurements (solid lines) conducted across the Fulford fault zone (5, Fig. 1). The table on the left lists the average magnetic field in each of the zones identified. Also shown are the magnetic susceptibility values (open circles). The vertical line indicates the mapped fault location.

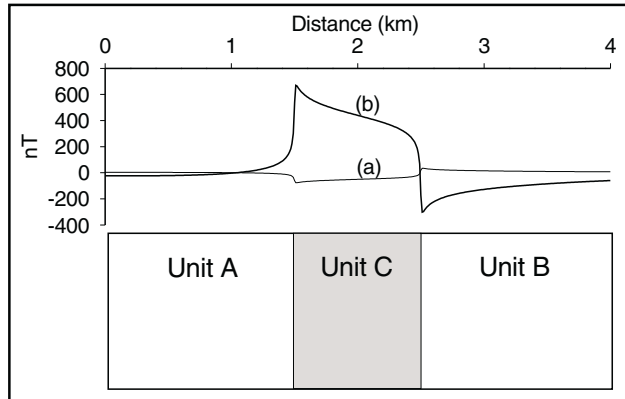


**Figure 7.** Synthetic models. Units A and B in lower figure have a susceptibility of  $4 \times 10^{-3}$  SI. When unit C has a susceptibility of  $1 \times 10^{-3}$  SI, the anomaly shown in **a)** upper figure is generated; when unit C has a susceptibility of  $20 \times 10^{-3}$  SI, the anomaly shown in **b)** upper figure is generated.